Research Square

Preprints are preliminary reports that have not undergone peer review.
They should not be considered conclusive, used to inform clinical practice,
or referenced by the media as validated information.

Prediction of historical, current and future configuration of Gymnadenia orchidis 1 based on the optimized MaxEnt in the Qinghai-Tibet Plateau

Ming LI
Yangtze University
Yi Zhang
Yangtze University
Tongxin Wang
Yangtze University
Chu WU
Yangtze University
Xiujuan Zhang (zxj510@yangtzeu.edu.cn)
Yangtze University
Junbang Wang
Institute of Geographic Sciences and Natural Resources Research

Research Article

Keywords: Suitability, Climate change, MaxEnt, Gymnadenia orchidis, Qinghai-Tibet Plateau

Posted Date: January 11th, 2024

DOI: https://doi.org/10.21203/rs.3.rs-3848112/v1

License: This work is licensed under a Creative Commons Attribution 4.0 International License.
Read Full License

Additional Declarations: No competing interests reported.

Prediction of historical, current and future configuration of *Gymnadenia orchidis* based on the optimized MaxEnt in the Qinghai-Tibet Plateau

Ming Li[1†], Yi Zhang[1†], Tongxin Wang[1], Chu Wu[1], Xiujuan Zhang[1*], Junbang Wang[2*]

[1] College of Horticulture & Gardening, Yangtze University, Jingzhou 434025, China

[2] National Ecosystem Science Data Center, Key Laboratory of Ecosystem Network Observation and Modeling, Institute of Geographic Sciences and Natural Resources Research, Chinese Academy of Sciences, Beijing 100101, China

[†] The authors contribute equally to this work.

***Corresponding author:** Xiujuan ZHANG: zxj510@yangtzeu.edu.cn; Junbang Wang: jbwang@igsnrr.ac.cn

Abstract: *Gymnosia orchidis* (*G. orchidis*) is a valuable Tibetan medicinal resource with significant medicinal, ecological, and economic value. However, the growth of *G. orchidis* is severely constrained by stringent natural conditions, leading to a drastic decline in its resources. Therefore, it is crucial to study the suitable habitat areas of *G. orchidis* to facilitate future artificial cultivation and maintain ecological balance. In this study, we investigated the suitable zones of *G. orchidis* based on 79 occurrence points in the Qinghai-Tibet Plateau (QTP) and 23 major environmental variables, including climate, topography, and soil type. We employed the Maximum Entropy model (MaxEnt) to simulate and predict the spatial distribution and configuration changes of *G. orchidis* during different time periods, including the last inter-glacial (LIG), the last glacial Maximum (LGM), the Mid-Holocene (MH), the present, and future scenarios (2041—2060 and 2061—2080) under three different climate scenarios (SSP126, SSP370, and SSP585). Our results indicated that annual precipitation (Bio12, 613—2466 mm) and mean temperature of the coldest quarter (Bio11, -5.8—8.5 °C) were the primary factors influencing the suitable habitat of *G. orchidis*, with a cumulative contribution of 78.5%. The precipitation and temperature during the driest season had the most significant overall impact. Under current climate conditions, the suitable areas of *G. orchidis* covered approximately 63.72×10^4/km², encompassing Yunnan, Gansu, Sichuan, and parts of Xizang provinces, with the highest suitability observed in the Hengduan, Yunlin, and Himalayan mountain regions. In the past, the suitable area of *G. orchidis* experienced significant changes during the Mid-Holocene, including variations in total area and centroid migration direction. In future scenarios, the suitable habitat of *G. orchidis* is projected to expand significantly under SSP370 (30.33%—46.19%), followed by SSP585 (1.41%—22.3%), while contraction is expected under SSP126. Moreover, the centroids of suitable areas exhibited multidirectional movement, with the most extensive displacement observed under SSP585 (100.38 km²). This research provides valuable insights for guiding the selection of introduced species, artificial cultivation, and resource conservation in the future, while also offering theoretical support for the protection of endangered species.

Keywords: Suitability; Climate change; MaxEnt; *Gymnadenia orchidis*; Qinghai-Tibet Plateau

1. Introduction

Gymnosia orchidis (*G. orchidis*) is a vulnerable species (VU) belonging to the Gymnadenia genus in the *Orchidaceae* family, It holds the highest extinction risk among numerous plant species (Barbara et al. 2004; luo et al. 2013). *G. orchidis*, known as "Wangla" in Tibetan medicine, possesses significant medicinal value, including the treatment of lung deficiency, bleeding, and cough (Wang et al. 2022). It also plays a crucial role in the combined treatment of type 2 diabetes (T2DM), where its tuberous root and pumpkin seeds are utilized (Wang and Wang 2022). However, research on *G. orchidis* has primarily focused on its pharmacological actions, with limited publications on predicting its potential suitable zones (Subiah et al. 2018). This knowledge gap is concerning given the species' longer growth cycle and reliance on wild resources, making it increasingly rare (Wang and Wang 2022; Xi et al. 2000). The wild resources of *G. orchidis* are continuously declining, with low production but increasing demand each year (Hisashi et al. 2004). Therefore, urgent attention is required for the conservation and cultivation of *G. orchidis*. *G. orchidis* has strong temporal and spatial heterogeneity when its suitability has been constantly expending from MH (Mid-Holocene) and the major distribution areas are located at Qinghai, Yunnan, Tibet, and Sichuan, in China, with its growth environments are hillside forests and alpine grasslands at altitude 2800—4100 meters, wide variation in the quality of regional resources (Li et al. 2023; XI, Lang 2000).

The Qinghai-Tibet Plateau (QTP), located at 67—105°E and 25—40°N, is a crucial region for *G. orchidis* distribution. With an average elevation of over 4000 meters above sea level, the QTP exhibits distinctive characteristics such as high altitude, diverse vegetation distribution, and pronounced zonal differences, giving rise to a unique alpine ecosystem (Feng et al. 2023; Li and Wang 2023; Ma et al. 2023b).Moreover, the QTP serves as an ecological screen that is highly sensitive and vulnerable to climate variability, not only in China but also in Asia as a whole (Ma et al. 2023a). Recent studies have indicated a warming and wetting trend in the QTP over the past 40 years, which is projected to continue. These changes not only impact the physiological and biochemical processes of various plant species, increasing the risk of extinction for endangered species like *G. orchidis*, but also have the potential to alter the global vegetation ecological pattern, posing significant threats to organism and ecosystem diversity (Wang et al. 2023a). Consequently, it is crucial to explore potential suitable areas for endangered species in the future to facilitate biodiversity protection and maintain ecosystem balance in this region (Wei et al. 2023).

To address this need, species distribution modeling (SDM) is employed as the primary method to simulate

suitable habitat areas and predict distribution changes based on environmental variables (Huang et al. 2020)., commonly used SDMs such as Genetic Algorithm for Rule-set Production (GARP), Climate and Expertise (Climex), Maximum Entropy model (MaxEnt) (Regan et al. 2021; Su et al. 2021). Among the SDM approaches, MaxEnt is widely used due to its simplicity, rapid processing, and high prediction accuracy, even with limited distribution points (Huang et al. 2023b; Kang et al. 2023; Xu et al. 2019). MaxEnt has good applications in predicting prehistoric geology and future climate scenarios and particularly suitable for predicting suitable areas for endangered species, afforestation tree species, and exotic tree species, as well as assessing their response to future climate change (He et al. 2023; Radosław et al. 2023; Wang et al. 2023b; Zhao et al. 2021).

This study focuses on *G. orchidis* and aims to simulate the current distribution pattern of its suitable areas in the QTP using MaxEnt. Furthermore, it seeks to predict the potential suitable areas in paleo and future time periods paleo consists of last inter-glacial (LIG, 140000 yr B.P), last glacial Maximum (LGM, 22000 yr B.P) and Mid-Holocene (MH, 6000 yr B.P); the future contains 2050s (2041—2060) and 2070s (2061—2080).The ultimate goal is to develop a numerical model that accurately predicts the suitable areas for *G. orchidis*, facilitating informed introductions and resource conservation efforts. This research has the potential to catalyze regional biodiversity conservation and contribute to the development of related industries.

2. Materials and methods

2.1. Species distribution data

The distribution data for *G. orchidis* were primarily obtained from the Global Biodiversity Information Facility (GBIF, http://www.gbif.org/) and supplemented with field investigations. The species specimens were accessed online through the Chinese Virtual Herbarium (CVH, http://www.cvh.ac.cn). To ensure the timeliness of the specimen data, we selected and recorded plant sample sites from GBIF within Continental China, using latitude and longitude coordinates. We then cross-referenced the distribution range of the studied species mentioned in relevant literature (Feng and Liu 2023; Ma and Huang 2023b) and supplemented the data with information from the second Qinghai-Tibet scientific survey. To reduce sampling bias, redundant distributed sample points were screened by establishing a 5×5 km buffer using ArcGIS 10.8. Within each buffer, one site was randomly retained as a representative point (Boria et al. 2014; Geue et al. 2020). A total of 79 documented records of *G. orchidis* presence in QTP were compiled and stored in a CSV format (Fig. 1).

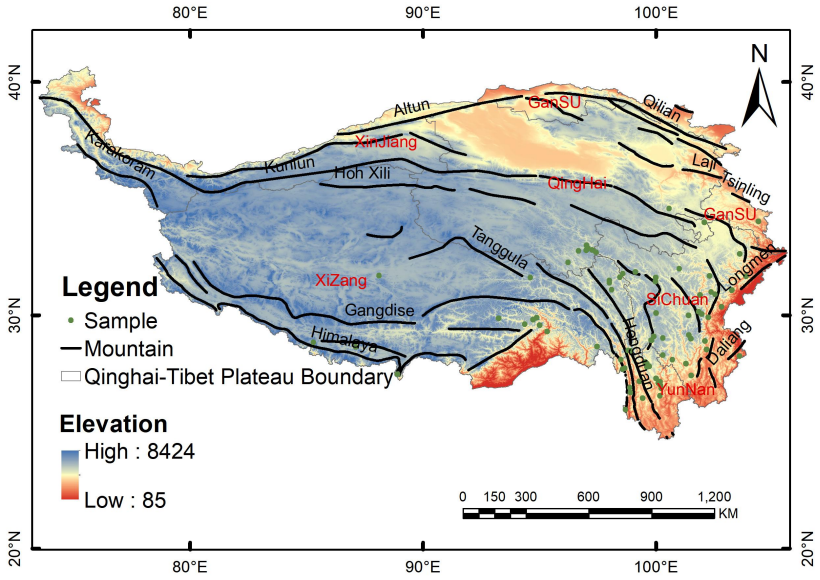


Fig. 1 Qinghai-Tibet Plateau distribution of *G. orchidis* sample points

2.2. Environmental variables

Considering the specific conditions of the research area, this study selected 23 environmental variables from climate, topography, and soil. Climate data, including the Last Interglacial (LIG), Last Glacial Maximum (LGM), Mid-Holocene (MH), current, and future climates, were obtained from the WorldClim Globe Climate Database (http://worldclim.org/) at a resolution of 2.5 arcminutes (ca. 5 km). The time period for the current climate data was 1970—2000, which was used to construct the initial model. Paleo-climate data (LIG, LGM, and MH) were generated using the Community Climate System Model version 4 (CCSM4). Future climate data were based on the BCC—CSM2—MR model, which underwent historical tests of CMIP6 and was used in future Shared Socio-economic Pathways (SSPs) scenario tests (Wu et al. 2019). Three scenarios under the SSPs were selected: SSP126 (Sustainability pathway), SSP370 (Medium emission path), and SSP585 (A path dominated by traditional fossil fuels). These scenarios were chosen for their high applicability to the current research and their ability to better evaluate temperature, precipitation, and atmospheric circulation (Keywan et al. 2016; Shi et al. 2023). The future time periods considered were the 2050s (averages for 2041—2060) and 2070s (averages for 2061—2080) (Alexander et al. 2016). Topographic variables such as slope and aspect were derived using surface analysis tools in ArcGIS. Soil type data were obtained from the Harmonized World Soil Database (HWSD, www.fao.org) and resampled into raster data with a resolution of 2.5 arcminutes (ca. 5 km) to ensure data consistency (He, Ma 2023; Jiao et al. 2023). The biological variables obtained as described above were spatially projected using the World Geodetic System (WGS 1984) (Kottarathu et al. 2022).

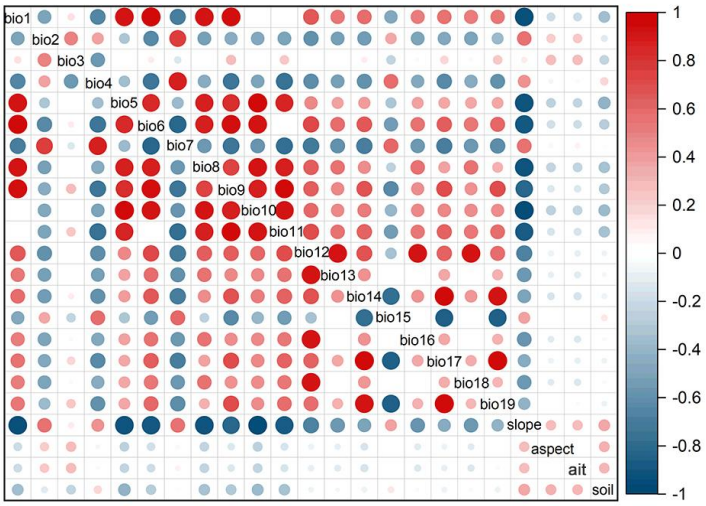


Fig. 2 Correlation diagram of environmental variables for the *G .orchidis*

To address potential multicollinearity issues and prevent overfitting of the model predictions, a Pearson correlation analysis was conducted on the environmental variables obtained from WorldClim (Kottarathu and Youngwook 2022). The correlation analysis aimed to identify variables that were strongly correlated with each other. Based on the results of the correlation analysis (Fig. 2), all the environmental variables were imported into the MaxEnt. Variables with zero contribution, as determined by the jackknife analysis, were removed. The remaining variables were further analyzed by considering their correlations. If two variables had a correlation coefficient greater than or equal to 0.8, only the variable with the highest contribution was retained. Ultimately, six variables were selected as the evaluation variables for the model: Annual precipitation (Bio12), Mean temperature of the coldest quarter (Bio11), Minimum temperature of the coldest month (Bio6), Temperature seasonality (Bio4), Aspect (Asp), and Precipitation of the coldest quarter (Bio19) (Table 1). These variables were deemed to have the most significant contribution to the model's predictions.

Table 1 Environment variables for driving MaxEnt

Code	Variables	Unit
Bio12	Annual precipitation	mm
Bio11	Mean temperature of coldest quarter	°C
Bio6	Min Temperature of coldest month	°C
Bio4	Temperature seasonality(standard deviation×100)	Dimensionless
Aspect	Aspect based on a digital elevation model	degree
Bio19	Precipitation of coldest quarter	mm

2.3. Construction, Optimization, and Evaluation of MaxEnt

In this study, the optimized MaxEnt was selected to overcome the complexity and limited portability of the default parameter settings in the initial model (Zhou et al. 2023b). To determine the optimal parameter combination, the ENMeval package in R 4.2.2 was utilized. The regularization multipliers (RM) were regrouped, ranging from 0.1 to 4.0 with 0.1 intervals, and the feature combination (FC) parameters were considered. The FC parameters included L (Linear), LQ (Quadratic), LQH, H (Fragmentation), LQHP (Product), and LQHPT (Threshold). These parameters were cross-combined to facilitate the evaluation of MaxEnt's complexity under different parameter combinations using R (Robert et al. 2014; Zhou and Li 2023b). A total of 240 combinations were adjusted using the ENMeval package. Subsequently, the best parameter combination was selected for modeling based on a delta.AICc= 0 (Jiao and Long 2023). The delta.AICc value was a measure of the difference in AICc (Akaike Information Criterion corrected for small sample sizes) between models, and a value of 0 indicated the best-fitting model in terms of complexity and goodness of fit. The selected parameter combination was presented in Table 2.

Table 2 MaxEnt optimized parameter setting by ENMeval

Type	FC	RM	Delta.AICc	Mean.OR10
default	LQHP	1	63.07	0.25
optimized	LQH	2.6	0	0.21

In this study, the MaxEnt was imported with screened occurrence data (* .csv) and environmental variables data (* .asc). The "Logistic" mode was selected as the output mode, which had the same parameter set as MaxEnt but was more adaptable (Phillips et al. 2008). To evaluate the predictive power of the models, independent training models were used. The "Bootstrap" method was chosen as the replicated run type, where 25% of the dataset was randomly selected as the test set, and the remaining 75% was used as the training set. This process was repeated 10 times to minimize errors in both the training and test data (Gebrewahid et al. 2020; Zheng et al. 2022). Sample points were randomly selected from a pool of 10,000 background grid cells, and the "Random seed" option was used to increase the randomness of the model. The plotting data were recorded for generating charts (Silva et al. 2019; Xu and Zhuo 2019). The remaining parameters were kept at their default values. The accuracy of the simulation results was assessed using the Receiver Operating Characteristic (ROC) curve, and the Area Under Curve (AUC) was calculated. The AUC measures the degree of

discrimination between sites where observations were present or absent. A higher AUC value closer to 1 indicates a more accurate model. The forecast results were divided into different intervals based on the AUC values, ranging from excellent (0.9—1.0) to fail (0.5—0.6) (HamadAmin et al. 2023; Huang and Ma 2020). After running the model, a suitability index was obtained, representing the range of potentially suitable distribution areas for *G. orchidis*. The suitability index values ranged from 0 to 1, with higher values indicating a higher likelihood of the species being present in that region. Based on the prediction of habitat suitability, the suitability areas were classified into four grades: not suitable (value≤ MTSPS), generally suitable (MTSPS< value≤ 0.4), moderately suitable (0.4< value≤ 0.6), and highly suitable (0.6< value) (Jiao and Long 2023). Furthermore, the SDM toolbox under the ArcGIS extensions was used to analyze the changes in the distribution area and the geometric center of the habitat under different climate change scenarios. This analysis aimed to detect the general trend of the offset in *G. orchidis* distribution

2.4. Application software and data resources

Digital Mountain Map obtained from Data set of Digital Mountain Map of China (2015) (Nan et al. 2022); MaxEnt software (USA) was downloaded at open source (http://biodiversity informatics.amnh.org/), Versions were 3.4.4. The version of SPSS (USA) was 27.0.

3. Results

3.1. Model validation and importance of environmental variables for prediction

The ROC curves generated from the MaxEnt indicated high performance in both the training set and the test set. The Area Under Curve (AUC) value for the training set was 0.939, while the AUC value for the test set was 0.959. These high AUC values, close to 1, suggested that the MaxEnt performed well in the current scenario. The model was able to accurately fit the species distribution data and provide reliable predictions (Fig. 3).

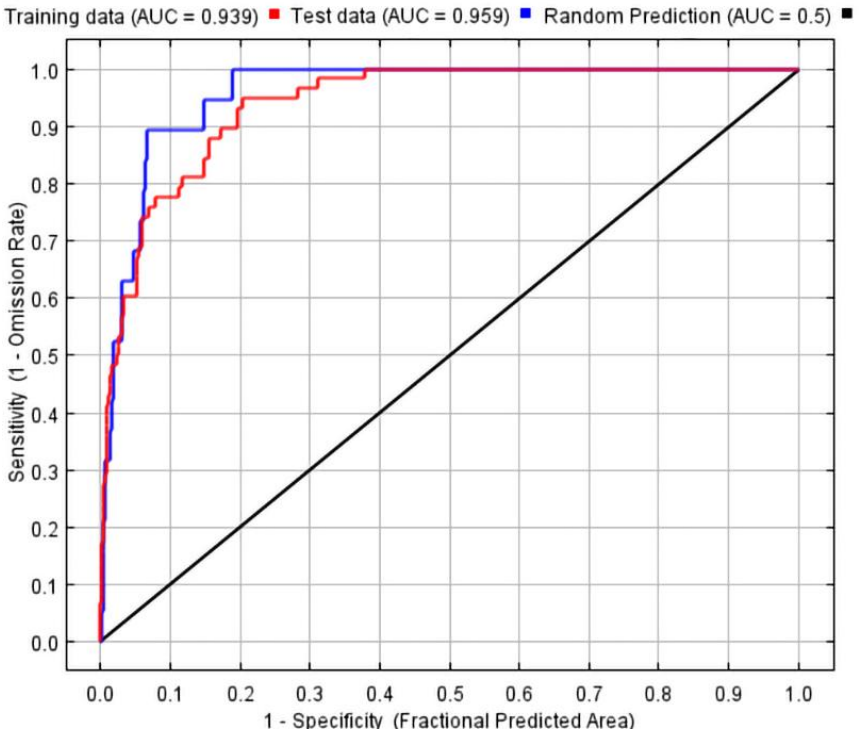


Fig. 3 Receiver operating characteristic curve with the area under the curve (AUC)

The jackknife test results provided insights into the key environmental factors influencing the distribution of *G. orchidis*. The top two variables identified were Annual Precipitation (Bio12) and Mean temperature of coldest quarter (Bio11). These two variables accounted for a cumulative contribution of 78.5%. Additionally, the accrued Permutation importance reached 90.1%, further confirming the dominance of Bio12 and Bio11 as significant environmental factors for *G. orchidis*. Furthermore, Bio6 (Minimum temperature of coldest month) and Bio4 (Temperature seasonality) accounted for up to 15.9% of the contribution, indicating that these variables were equally important for the growth and development of *G. orchidis*. This suggests that factors related to the coldest temperatures and temperature variations throughout the year play a crucial role in determining the suitable habitat for *G. orchidis* (Table 3).

Table 3 Contribution rate of environmental variables of *G. orchidis*

Variables	Percent contribution(%)	Permutation importance(%)
Bio12	55.1	16.8
Bio11	23.4	73.3
Bio6	8.1	0.1
Bio4	7.8	2.5
Aspect	3.8	4.1
Bio19	1.9	3.2

The Jackknife test results indicated that the training gain remained stable when each environmental variable was used in isolation, suggesting that these variables individually influenced the predictive ability of the MaxEnt for *G. orchidis*. The variables that affected the suitable area of *G. orchidis* were Bio6, Bio4, Bio19 (Precipitation of coldest quarter), Bio12, Bio11, and Aspect. Additionally, the training gain decreased when Bio19 and Aspect were not included, indicating that the predictive power of the model would be reduced if these variables were excluded. This suggested that Bio19 (Precipitation of coldest quarter) and Aspect had a profound impact on the suitability of *G. orchidis*. The inclusion of these variables in the model improves its ability to accurately predict the suitable habitat for *G. orchidis* (Fig. 4).

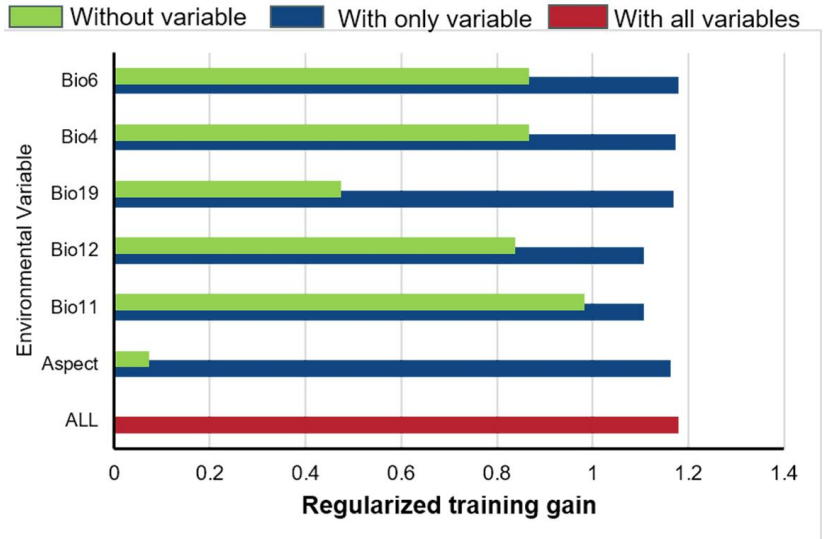


Fig. 4 Jackknife plot for training gain

3.2. Simulated Current Potentially Suitable Distribution

The response curve of *G. orchidis* provided insights into the range of habitat suitability based on the current climatic conditions. According to the response curve, *G. orchidis* showed a preference for specific ranges of environmental variables. For Annual Precipitation (Bio12), the preferred range was between 613 mm and 2466 mm. This indicated that *G. orchidis* thrives in areas with moderate to high levels of annual

precipitation. The Mean temperature of the coldest quarter (Bio11) ranged from -5.8 °C to 8.5 °C. *G. orchidis* showed a preference for areas with relatively mild temperatures during the coldest quarter of the year. The Temperature seasonality (Bio4) ranged from 437 to 648. *G. orchidis* exhibited a preference for areas with a certain level of temperature variation throughout the year. The Minimum temperature of the coldest month (Bio6) ranged from -14.0 °C to 3.7 °C. *G. orchidis* showed a preference for areas where the minimum temperature during the coldest month falls within this range. Lastly, for Precipitation of the coldest quarter (Bio19), *G. orchidis* preferred areas with a precipitation level exceeding 11 mm. These ranges provided valuable information for understanding the habitat preferences of *G. orchidis* under current climatic conditions (Fig. 5).

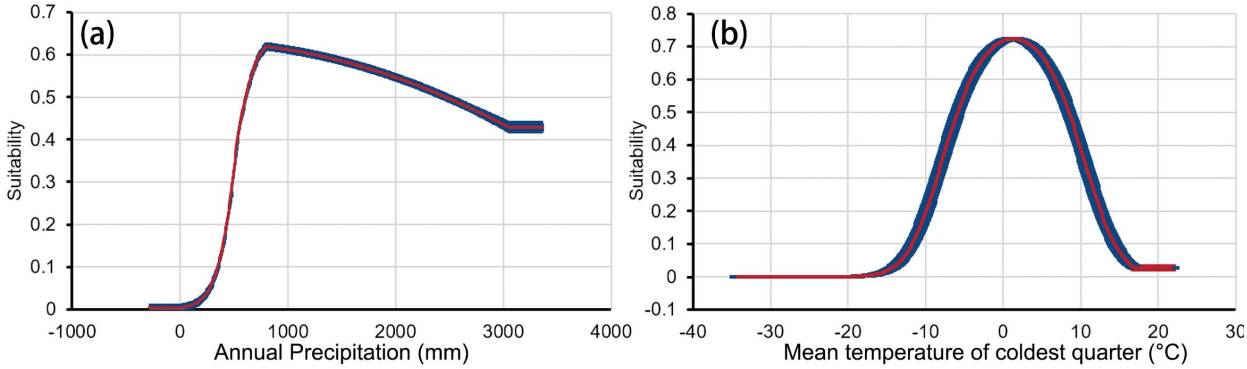


Fig. 5 Response curves of *G. orchidis*. (a) Annual Precipitation (b) Mean temperature of coldest quarter

Based on the prediction results of MaxEnt, we used ArcGIS techniques to reclassify and visual analytics for the potentially suitable areas of *G. orchidis* in the QTP (Fig. 6, 7). Under the current climatic conditions, total potential suitable areas of *G. orchidis* reached out to about $63.72\times10^4/km^2$ (Table 3), the proportion of suitable area in high, moderate, general and not suit were 6.55%, 10.33% ,7.33% and 76.01%, respectively.

Table 4 Change of current potential suitable area of *G. orchidis*

Year	Suitable area/$\times10^4/km^2$			
	Not suitable	Generally suitable	Moderately suitable	Highly suitable
1970-2000	201.92	18.88	27.44	17.4

The potential distribution of *G. orchidis* was found to be primarily located in the southeast region of the QTP, specifically within the latitude range of 25° N to 35° N and longitude range of 80° E to 105° E. This area includes the provinces of Yunnan, Sichuan, Gansu, and parts of Xizang (Tibet) (Table 3). Within this region, the highly suitable areas for *G. orchidis* were predominantly concentrated in the northern part of Yunnan, southern part of Tibet, and eastern regions of Sichuan and Gansu. These highly suitable areas were distributed along

mountain ranges such as Hengduan, Yunlin, and the Himalayas. These regions exhibit the most favorable conditions for the growth and development of *G. orchidis*. Moderately and generally suitable areas, which also provided suitable habitat for *G. orchidis*, covered a broader area including the provinces of Yunnan, Gansu, Sichuan, and southern Tibet (Fig. 6). These regions may had slightly less optimal conditions compared to the highly suitable areas but still support the growth and survival of *G. orchidis*. Overall, the study identified specific geographic regions within the southeast of the QTP as the potential distribution range for *G. orchidis*, with highly suitable areas concentrated in certain mountainous regions and moderately and generally suitable areas covering a larger extent of the studied provinces.

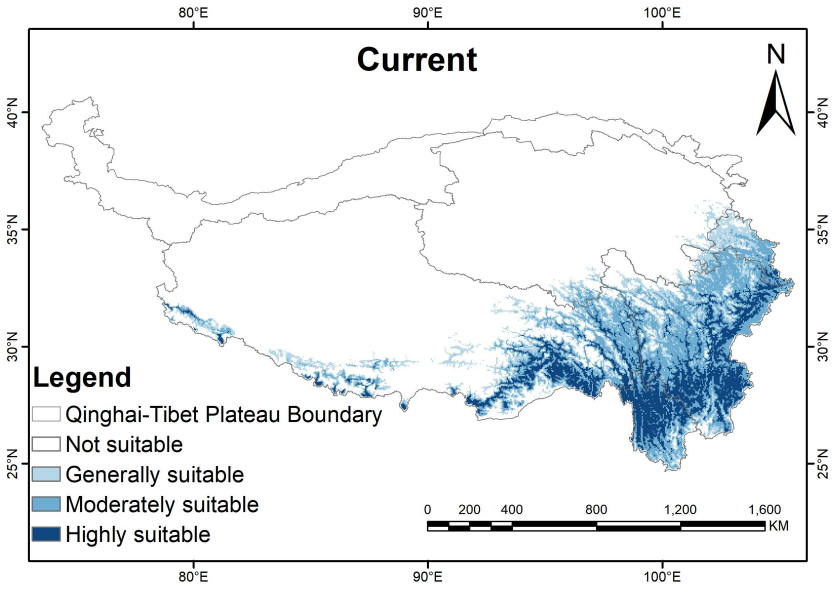


Fig. 6 Distribution of potential suitable areas of the QTP region of *G.orchidis* under the current climate

3.3. Predicted Past and Future Potentially Suitable Distribution

The potential suitable area for *G. orchidis* in the past and future remains primarily in the southeast region of the QTP, including the provinces of Yunnan and parts of Tibet, Sichuan, and Gansu. The highly suitable areas continue to be distributed along mountain ranges such as Hengduan, Yunlin, Longmen, and others. During the glacial periods, such as the Last Interglacial (LIG) and Last Glacial Maximum (LGM), there was less suitability for *G. orchidis* due to the harsh environmental conditions associated with glaciation. However, there was an increase in highly suitable areas during the LGM, primarily focused on mountain ranges. This suggested that *G. orchidis* may had found refuge in these mountainous regions during the glacial periods. In contrast, during the post-glacial period (MH, or Mid-Holocene), the suitable area of *G. orchidis* expanded to the northwest from its previous range. However, the highly suitable areas decreased in this period, and

non-mountainous areas gradually became suitable, although more in a generally suitable range. Looking into the future under three scenarios, the suitable area with high suitability for *G. orchidis* was projected to further expand to the northwest of the QTP, specifically in the Qinghai province. However, the southern part of Yunnan is expected to experience a loss of suitability for *G. orchidis* (Fig. 7, 8). These findings suggested that the potential distribution of *G. orchidis* was influenced by past climatic changes and was projected to shift in response to future climate scenarios. The mountainous regions continued to be crucial for the highly suitable habitat of *G. orchidis*, while other areas may became generally suitable or experience changes in suitability

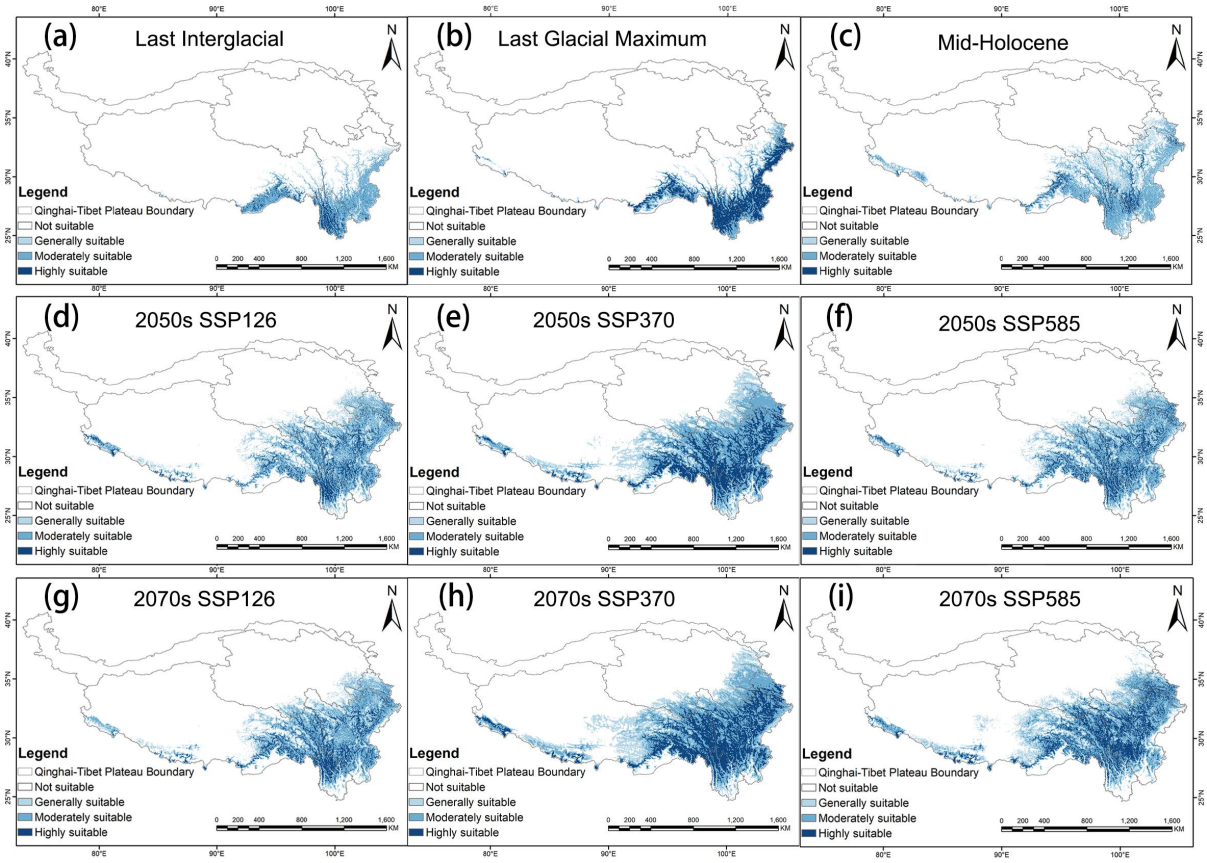


Fig. 7 Distribution of potential suitable areas of the QTP region of *G. orchidis* under different climate change scenarios in the future (a) The potential geographical distribution of *G. orchidis* under the Last interglacial (b) The potential geographical distribution of *G. orchidis* under the Last Glacial Maximum (c) The potential geographical distribution of *G. orchidis* under the Mid-Holocene (d) The potential geographical distribution of *G. orchidis* under the SSP126 in the 2050s (e) The potential geographical distribution of *G. orchidis* under the SSP370 in the 2050s (f) The potential geographical distribution of *G. orchidis* under the SSP585 in the 2050s (g) The potential geographical distribution of *G. orchidis* under the SSP126 in the 2070s (h) The potential geographical distribution of *G. orchidis* under the SSP370 in the 2070s (i) The potential geographical distribution of *G. orchidis* under the SSP370 in the 2070

The suitable area for *G. orchidis* had shown a remarkable growth trend from the past to the future. In the past, the suitable area was increased from 32.56% to 65.79%, only 32.56% in LIG and covered an area of $26.32\times10^4/km^2$. However, in the present time, the suitable area has increased to 65.79%, covering a much larger area of $63.72\times10^4/km^2$. Looking at the future scenarios, the geographic distribution of *G. orchidis* was projected to expand and contract, but the expansion was expected to outweigh the contraction. Among the three scenarios,

SSP370 showed the highest rate of expansion, ranging from 34.07% to 52.2%, while the contraction rate was relatively low, ranging from 3.74% to 6.01%. SSP585 also exhibited expansion, with a range of 14.69% to 38.21%, but there was also a noticeable loss rate and contraction ranging from 1.44% to 22.3%. Overall, there were no significant changes in the overall suitability compared to SSP370. In the SSP126 scenario, there was not much change in the suitability area, but there was less contraction ranging from 1.77% to 2.21%. In summary, the suitable area for *G. orchidis* showed promising prospects in the future. Among the scenarios, SSP370 provided the best growth environment for *G. orchidis*, followed by SSP585, while SSP126 was the least favorable scenario (Fig. 7, 8, 9, Table 5).

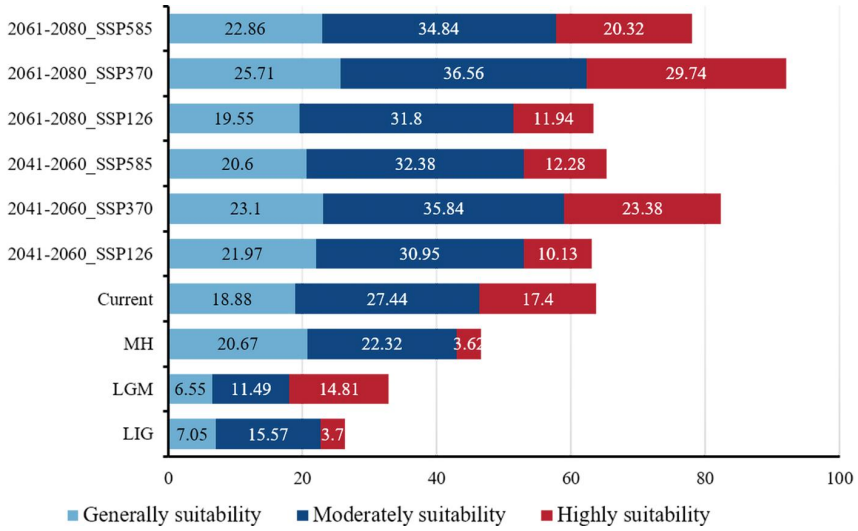


Fig. 8 Potential suitable area of *G. orchidis* under different scenarios ($\times 10^4/km^2$)

Table 5 Suitable distribution of *G. orchidis* under different climate change scenarios

Year	Area/$\times 10^4 km^2$				Change rate/%			
	Increase	Reserved	Last	Change	Increase	Reserved	Last	Change
LIG	41.92	26.12	1.97	39.95	65.79	40.99	3.09	62.70
LGM	33.92	34.09	1.28	32.64	53.23	53.50	2.01	51.22
MH	20.75	47.29	2.14	18.61	32.56	74.22	3.36	29.20
2050s_SSP126	7.93	58.70	9.34	-1.41	12.45	92.12	14.66	-2.21
2050s_SSP370	21.71	63.00	2.38	19.33	34.07	98.87	3.74	30.33
2050s_SSP585	9.36	59.58	8.46	0.90	14.69	93.50	13.28	1.41
2070s_SSP126	7.59	59.32	8.72	-1.13	11.91	93.09	13.68	-1.77
2070s_SSP370	33.26	63.72	3.83	29.43	52.20	100.00	6.01	46.19
2070s_SSP585	24.35	57.91	10.14	14.21	38.21	90.88	15.91	22.30

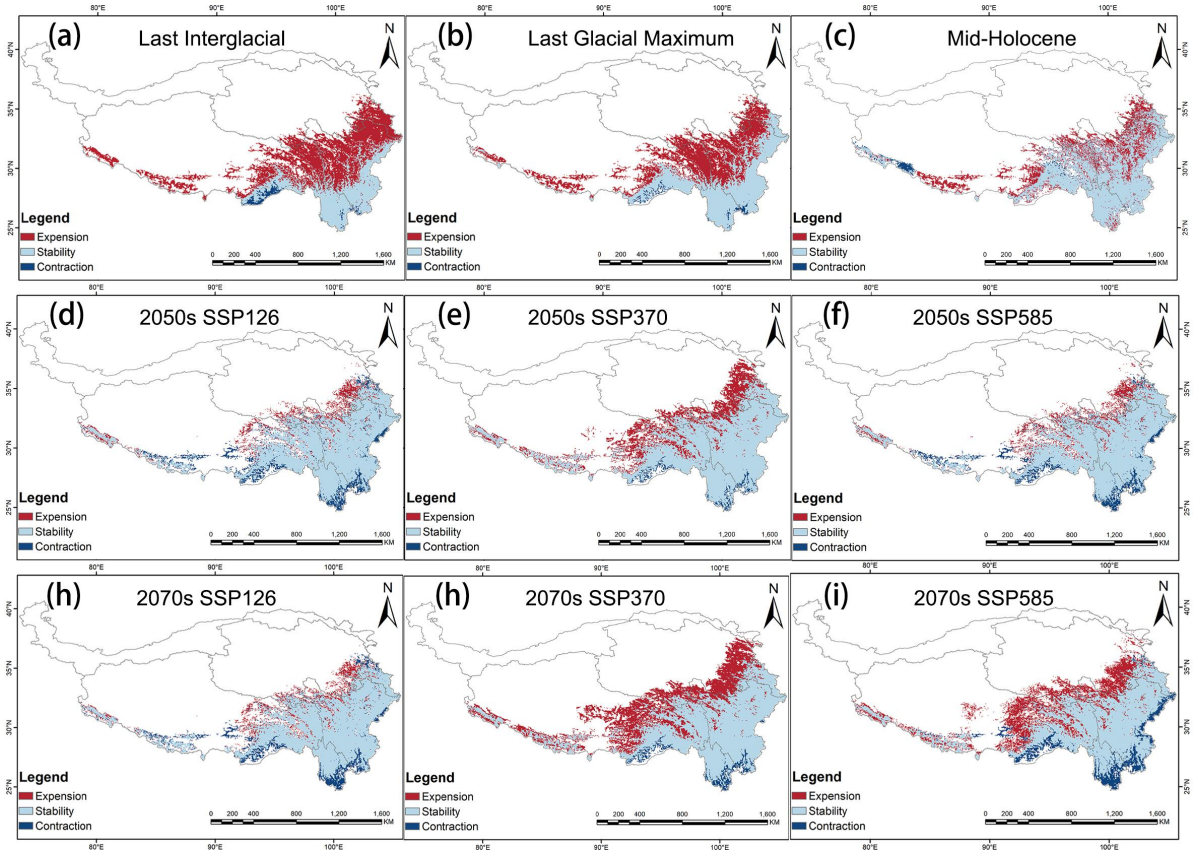


Fig. 9 Spatial variation of potential habitat of *G. orchidis* under different climate scenarios compared with modern climate scenarios (a) area changed under the Last interglacial (b) area changed under the Last Glacial Maximum (c) area changed under the Mid-Holocene (d) area changed under the SSP126 in the 2050s (e) area changed under the SSP370 in the 2050s (f) area changed under the SSP585 in the 2050s (g) area changed under the SSP126 in the 2070s (h) area changed under the SSP370 in the 2070s (i) area changed under the SSP585 in the 2070s

3.4. Shift of distribution centroid under different climate condition

The geographic coordinate point of the centroid of the suitable region for *G. orchidis* was located in the western part of Basu County (96° 42' 01″ E, 30° 06' 13″ N). In the past, the centroid of *G. orchidis* exhibited a remarkable tendency to transfer in a northwest direction, with a migration distance of 244.5/km. Specifically, during the glacial periods, the centroid showed an overall northward migration. However, during the Mid-Holocene (MH), the centroid shifted westward to coordinates 98° 05' 34″ E, 30° 00 '14″ N. Under the future climate scenarios, the migration direction of the centroid showed significant differences. In the SSP126 scenario, the centroid moved towards the northeast, indicating a trend of reverse migration in the medium term, with the farthest migration distance of 104.96/km compared to other scenarios. In the SSP370 scenario, the

centroid shifted westwards to Bomi County 96° 15' 34 ″E, 30° 02' 39″ N), with the least offset distance of 42.92/km. In the SSP585 scenario, the center point initially moved towards the north but eventually shifted northeastwards to Chaya County (97° 36' 09″ E, 30° 34' 05″ N), which was closed to the centroids in the SSP126 scenario. These migration patterns of the centroid point indicate the shifting distribution of suitable habitat for *G. orchidis* under different future climate scenarios (Table 6, Fig. 10).

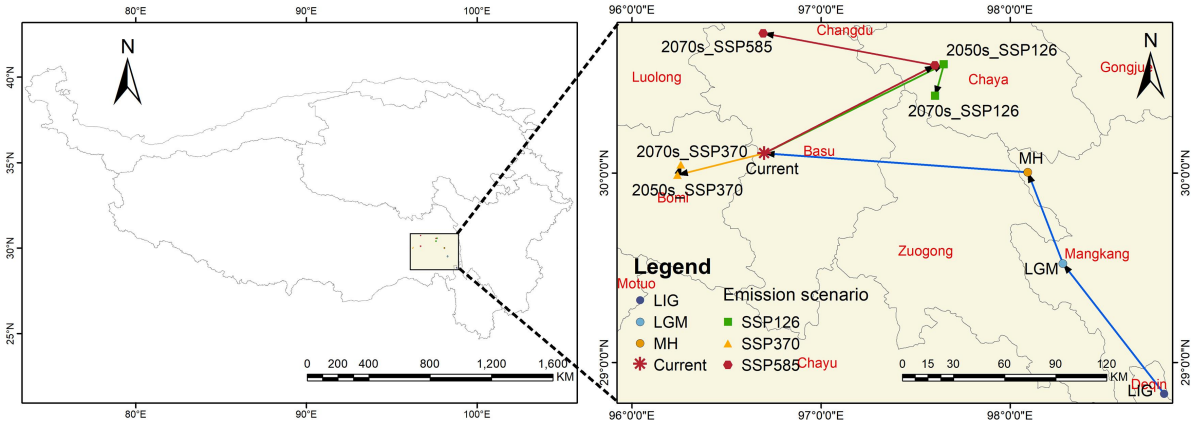


Fig. 10 Centroid transfer in potential suitable areas of *G. orchidis* under different climate

Table 6 Centroid coordinates and migration distance

Climate scenario	Year	Longitude	Latitude	Migration distance/km
	LIG	98°48'49″E	28°50'03″N	244.55
	LGM	98°16'44″E	29°31'19″N	165.47
	MH	98°05'34″E	30°00'14″N	134.48
	Current	96°42'01″E	30°06'13″N	0.00
SSP126	2050s	97°38'56″E	30°34'24″N	104.96
	2070s	97°36'12″E	30°24'25″N	93.07
SSP370	2050s	96°14'32″E	29°59'24″N	45.85
	2070s	96°15'34″E	30°02'39″N	42.92
SSP585	2050s	97°36'09″E	30°34'05″N	100.83
	2070s	96°41'42″N	30°44'13″N	70.42

4. Discussion

Hydrothermal conditions have been identified as the most important variables influencing the geographical distribution of plants, particularly terrestrial plants (Shi and Wang 2023). These conditions also play a key role in explaining the association between species richness and terrain (Odland et al. 2006). In our study, we found that Annual Precipitation (Bio12) and Mean temperature of coldest quarter (Bio11) were the dominant variables influencing the distribution of *G. orchidis*. This suggests that temperature and rainfall are the driving mechanisms for *G. orchidis*. Secondary variables such as Min Temperature of coldest month (Bio6), Temperature seasonality (Bio4), and Precipitation of coldest quarter (Bio19) further indicate that rainfall and temperature changes during the coldest quarter can influence the growth of *G. orchidis*. These findings align with the overall habitat characteristics of the *Orchidaceae* family (Hu et al. 2022) (Table 1). The results of MaxEnt indicate that *G. orchidis* has a limit threshold for cold and drought resistance at -14.0 °C and 11 mm, respectively. The species also shows a preference for southern slopes and an annual precipitation of 900 mm. These findings are consistent with previous research on plants of the *Orchidaceae* family (Acharya et al. 2011). Studies by (LI et al. 2019; Negi et al. 2021; Pramod et al. 2023) have suggested that the mountains on the southern slope of the study area experience higher temperatures and precipitation compared to the northern

slope. This indicates that the southern slope provides a sheltered environment to resist extreme cold conditions, which may be related to the diverse climate types in this region (Hu and Wei 2022). It is important to note that this study focused solely on the influence of climate, topography, and soil type on species distribution and did not consider biological factors such as interspecific relationships and anthropogenic forcing. Other factors, including genetic variation and soil environments, should be considered in future studies (Abla et al. 2023; Henderson et al. 2023; Hu and Wei 2022; Shi and Wang 2023; Zhang et al. 2019). Therefore, further research is needed to explore the dominant factors affecting *G. orchidis*.

The moderate and high mountainous areas with high precipitation, temperature, and humidity provide suitable habitats for rare species (Zhou et al. 2023a). Our study predicts that the potentially suitable areas for *G. orchidis* will vary under different climate scenarios over time, showing significant fluctuations in suitability. The MaxEnt results indicate that the distribution range of *G. orchidis* along mountains such as Henduan, Yunlin, and Longmen has constantly increased, especially during the MH when increased precipitation driven by solar radiation (Feng and Liu 2023). Previous studies (Li and Wang 2023) have also suggested that terrestrial herbs gradually dominated the QTP during the MH. The northwestward movement of the centroids further indicates the expansion of the suitable area for *G. orchidis* (Fig. 10). During the glacial period, the suitability for *G. orchidis* was reduced, likely due to the extensive ice coverage on the QTP (Huang et al. 2023a). The increase in highly suitable areas of *G. orchidis* during the LGM was more likely attributed to the southern slope of the mountains being reconstructed as a glacial refuge for *G. orchidis* (Pramod and F. 2023). Under different future scenarios, the suitable areas for *G. orchidis* continue to expand towards the northwest, including the provinces of Qinghai and Tibet, especially in the SSP370 scenario (with a temperature rise of 3.6 °C by the year 2100), where the expansion ratio reaches 46.19%. However, there is a loss of suitable areas in the SSP126 scenario (with a temperature rise of 1.8 °C by the year 2100), with contraction areas mainly concentrates in the Himalayas, possibly due to reduced precipitation (Acharya and Vetaas 2011; Wang et al. 2023c). Significant changes are observed in the SSP585 scenario (with a temperature rise of 4.4 °C by the year 2100), with the rate of change in suitable areas ranging from 1.4% to 22.3%. The centroid of *G. orchidis* in the 2050s approaches the centroid of the SSP126 scenario in the 2070s, indicating that the climatic conditions of the SSP126 scenario in the 2070s may be similar to those in the 2050s under the SSP585 scenario on the QTP . The multidimensional migration of centroids also suggests that changes in suitability may be influenced by carbon dioxide emissions (Alexander, Katherine 2016; IPCC 2022; Wu and Lu 2019). Increased CO_2 concentrations can improve the

survival of *G. orchidis* and align with the future growth trend of the *Orchidaceae* family as a whole (Hu and Wei 2022). However, human activities can disrupt suitable areas and force species migration, which is a complex issue. If a suitable environment is not found during the migration process, *G. orchidis* may be at risk of extinction (Faramarzi et al. 2023; Zhou and Li 2023a). As an extremely rare and environmentally sensitive Tibetan medicinal resource, the habitat conditions of *G. orchidis* are scarce and difficult to recover once lost. Therefore, active measures should be taken to reduce emissions and protect existing habitats.

ENMeval, as a criterion for quantitative evaluations of ecological niche models (ENMs), is widely used in optimizing MaxEnt to avoid multicollinearity and improve the accuracy of predictions. In our study, we utilized optimized MaxEnt to simulate and predict the suitability of *G. orchidis* under different scenarios. The high values of AUC (Area Under the Curve) greater than 0.9 indicate excellent predictive performance. However, it is important to note that MaxEnt are based solely on existing data, which may span a large period of time. They may lack consideration for actual conditions such as biological interactions, genetic variability, and species dispersal capacity, which can result in a wider prediction range for species distribution areas (Abla and Pallarés 2023). Therefore, future studies could further refine the model and incorporate more field validation to obtain more comprehensive details about the species, leading to better conservation assessments.

5. Conclusion

In this study, the Optimized MaxEnt was used to analyze the changes in the distribution pattern of *G. orchidis* in ancient and modern periods and make predictions for suitable areas under multiple future scenarios. The results highlighted that annual precipitation (Bio12) and mean temperature of the coldest quarter (Bio11) were the dominant factors, accounting for 55.1% and 23.4% of the influence, respectively. The range of Bio12 varied from 613 mm to 2466 mm, while Bio11 ranged from -5.8 °C to 8.5 °C. The study revealed a significant expansion of the suitable areas for *G. orchidis* from the past to the future. In the past, mountains such as Henduan, Yunlin, and Longmen served as glacial shelters for *G. orchidis*, and the centroids of its distribution shifted northwards. Under the future scenarios, there was a substantial expansion in the SSP370 scenario (30.33% to 46.19%), followed by the SSP585 scenario (1.41% to 22.3%). However, there was a contraction in suitable areas under the SSP126 scenario. The centroids of *G. orchidis* exhibited multi-directional movement, with the greatest distance observed in the SSP585 scenario (100.38/km). In summary, *G. orchidis* is expected to have better prospects in the future, but it is crucial to preserve its suitable habitats and avoid human-induced

377 destruction. The conservation of *G. orchidi*s not only has profound impacts on economic development but also
378 plays a crucial role in safeguarding biodiversity and maintaining the stability of ecosystem structures worldwide.

379 **References**

380 Abla B, Pallarés S, Nard B et al (2023) Towards the identification of hotspots of freshwater biodiversity
381 in North-Western Africa: A case study using species distribution models for water beetles in
382 Morocco. Global Ecology and Conservation 43:
383 e02441.https://doi.org/10.1016/j.gecco.2023.e02441

384 Acharya KP, Vetaas OR, Birks HJB (2011) Orchid species richness along Himalayan elevational
385 gradients. Journal of Biogeography 38:
386 1821-1833.https://doi.org/10.1111/j.1365-2699.2011.02511.x

387 Alexander P, Katherine C, Shinichiro F et al (2016) Land-use futures in the shared socio-economic
388 pathways. Global Environmental Change 42:
389 331-345.https://doi.org/10.1016/j.gloenvcha.2016.10.002

390 Barbara G, Ann S, Ferry JWS et al (2004) Epiphytism and pollinator specialization: drivers for orchid
391 diversity? Philosophical transactions of the Royal Society of London. Series B, Biological sciences
392 359: 1523-1535.https://doi.org/10.1098/rstb.2004.1529

393 Boria RA, Olson LE, Goodman SM et al (2014) Spatial filtering to reduce sampling bias can improve the
394 performance of ecological niche models. Ecological Modelling 275:
395 73-77.https://doi.org/10.1016/j.ecolmodel.2013.12.012

396 Faramarzi M, Isselstein J (2023) Assessing the response of rare and common plant species to human
397 induced rangeland degradation at a landscape scale in western Iran. Land Degradation &
398 Development 34: 5042-5054.https://doi.org/10.1002/ldr.4828

399 Feng SN, Liu XQ, Li K et al (2023) Quantitative precipitation reconstruction since mid-Holocene from
400 northeastern Tibetan Plateau: Implications for interplay between Asian summer monsoon and
401 Westerlies. Catena 233: 107521.https://doi.org/10.1016/j.catena.2023.107521

402 Gebrewahid Y, Abrehe S, Meresa E et al (2020) Current and future predicting potential areas of
403 Oxytenanthera abyssinica (A. Richard) using MaxEnt model under climate change in Northern
404 Ethiopia. Ecological Processes 9: 476-487.https://doi.org/10.1186/s13717-019-0210-8

405 Geue JC, Thomassen HA (2020) Unraveling the habitat preferences of two closely related bumble bee
406 species in Eastern Europe. Ecology and Evolution 10: 4773-4790.https://doi.org/10.1002/ece3.6232

407 HamadAmin BA, Khwarahm NR (2023) Mapping Impacts of Climate Change on the Distributions of

Two Endemic Tree Species under Socioeconomic Pathway Scenarios (SSP). Sustainability 15: 5469.https://doi.org/10.3390/su15065469

He YL, Ma JM, Chen GS (2023) Potential geographical distribution and its multi-factor analysis of Pinus massoniana in China based on the maxent model. Ecological Indicators 154: 110790.https://doi.org/10.1016/j.ecolind.2023.110790

Henderson AF, A.Santoro J, Kremer P (2023) Impacts of spatial scale and resolution on species distribution models of American chestnut (Castanea dentata) in Pennsylvania, USA. Forest Ecology and Management 529: 120741.https://doi.org/10.1016/j.foreco.2022.120741

Hisashi M, Toshio M, Haihui X et al (2004) Antiallergic phenanthrenes and stilbenes from the tubers of Gymnadenia conopsea. Planta medica 70: 847-855.https://doi.org/10.1055/s-2004-827234

Hu HW, Wei YQ, Wang WY et al (2022) Richness and distribution of endangered orchid species under different climate scenarios on the Qinghai-Tibetan Plateau. Frontiers in Plant Science 13: 948189-948189.https://doi.org/10.3389/fpls.2022.948189

Huang MP, Huang GP, Fan HZ et al (2023a) Influence of Last Glacial Maximum legacies on functional diversity and community assembly of extant Chinese terrestrial vertebrates. The Innovation 4: 100379-100379.https://doi.org/10.1016/J.XINN.2023.100379

Huang XT, Ma L, Chen CB et al (2020) Predicting the Suitable Geographical Distribution of Sinadoxa Corydalifolia under Different Climate Change Scenarios in the Three-River Region Using the MaxEnt Model. Plants 9: 1015.https://doi.org/10.3390/plants9081015

Huang ZM, Lu YL, Meng WQ et al (2023b) Study on suitability assessment of waterbird habitats along the Bohai Rim. Ecological Indicators 150: 110229.https://doi.org/10.1016/J.ECOLIND.2023.110229

IPCC, 2022. Climate Change 2022: Mitigation of Climate Change. *Contribution of Working Group III to the Sixth Assessment Report of the Intergovernmental Panel on Climate Change* [J.S. P.R. Shukla, R. Slade, A. Al Khourdajie, R. van Diemen, D. McCollum, M. Pathak, S. Some, P. Vyas, R. Fradera, M. Belkacemi, A. Hasija, G. Lisboa, S. Luz, J. Malley, (eds.)]. Cambridge University Press.,Cambridge, UK and New York, NY, USA.https://doi.org/10.1017/9781009157926

Jiao XY, Long M, Li JY et al (2023) Reconstructing the Invasive History and Potential Distribution Prediction of Amaranthus palmeri in China. Agronomy 13: 2498.https://doi.org/10.3390/agronomy13102498

Kang JF, Liu MS, Qu MK et al (2023) Identifying the potential soil pollution areas derived from the metal mining industry in China using MaxEnt with mine reserve scales (MaxEnt_MRS). Environmental Pollution 329: 121687-121687.https://doi.org/10.1016/J.ENVPOL.2023.121687

Keywan R, Vuuren DPv, Elmar K et al (2016) The Shared Socioeconomic Pathways and their energy, land use, and greenhouse gas emissions implications: An overview. Global Environmental Change 42: 153-168.https://doi.org/10.1016/j.gloenvcha.2016.05.009

Kottarathu KR, Youngwook K, Taoufik K (2022) Incorporating satellite remote sensing for improving potential habitat simulation of Prosopis cineraria (L.) Druce in United Arab Emirates. Global Ecology and Conservation 37: e02167.https://doi.org/10.1016/J.GECCO.2022.E02167

LI LL, LI J, CHEN HM et al (2019) Diurnal Variations of Summer Precipitation over the Qilian Mountains in Northwest China. Journal of Meteorological Research 33: 18-30.https://doi.org/10.1007/s13351-019-8103-4

Li WJ, Wang NN, Liang C et al (2023) Regional peculiarities in the importance of precipitation and temperature on mid-to-late Holocene arboreal degradation on the eastern Tibetan Plateau. Global and Planetary Change 229: 104252.https://doi.org/10.1016/J.GLOPLACHA.2023.104252

luo Y, Li DZ (2013) Flora of China. Science Press, China. https://doi.org/CNKI:SUN:YOKE.0.2013-06-012

Ma XY, Wei ZF, Wang YL et al (2023a) Temperature and Climatic Seasonality Affecting C3 Versus C4 Plants Since the Last Deglacial on the Northeastern Tibetan Plateau. Geochemistry Geophysics Geosystems 24: e2022GC010847.https://doi.org/10.1029/2022GC010847

Ma Y, Huang XD, Yang XL et al (2023b) Mapping snow depth distribution from 1980 to 2020 on the tibetan plateau using multi-source remote sensing data and downscaling techniques. ISPRS Journal of Photogrammetry and Remote Sensing 205: 246-262.https://doi.org/10.1016/J.ISPRSJPRS.2023.10.012

Nan X, Li A, Deng W, 2022. Data set of "Digital Mountain Map of China" (2015), A Big Earth Data Platform for Three Poles.

Negi SV, Tiwari CD, Singh L et al (2021) Review and synthesis of climate change studies in the Himalayan region. Environment, Development and Sustainability 24: 10471-10502.https://doi.org/10.1007/S10668-021-01880-5

Odland A, Birks HJB (2006) The altitudinal gradient of vascular plant richness in Aurland, western Norway. Ecography 22: 548-566.https://doi.org/10.1111/j.1600-0587.1999.tb01285.x

Phillips SJ, Dudík M (2008) Modeling of species distributions with Maxent: new extensions and a comprehensive evaluation. Ecography 31: 161-175.https://doi.org/10.1111/j.0906-7590.2008.5203.x

Pramod A, F. MJ (2023) Aerosol–precipitation elevation dependence over the central Himalayas using cloud-resolving WRF-Chem numerical modeling. Atmospheric Chemistry and Physics 23: 1019-1042.https://doi.org/10.5194/ACP-23-1019-2023

Radosław P, Sonia P-D, Andrzej MJ et al (2023) Predicted range shifts of alien tree species in Europe. Agricultural and Forest Meteorology 341: 109650.https://doi.org/10.1016/J.AGRFORMET.2023.109650

Regan E, Ivan R, Gilson C et al (2021) Comparing, evaluating, and combining statistical Species Distribution Models and CLIMEX to forecast the distributions of emerging crop pests. Pest management science 78: 671-683.https://doi.org/10.1002/PS.6677

Robert M, Peter JG, Mariano SG et al (2014) ENM eval: An R package for conducting spatially independent evaluations and estimating optimal model complexity for Maxent ecological niche models. Methods in Ecology and Evolution 5: 1198-1205.https://doi.org/10.1111/2041-210X.12261

Shi XD, Wang JW, Zhang L et al (2023) Prediction of the potentially suitable areas of Litsea cubeba in China based on future climate change using the optimized MaxEnt model. Ecological Indicators 148: 110093.https://doi.org/10.1016/j.ecolind.2023.110093

Silva C, Leiva F, Lastra J (2019) Predicting the current and future suitable habitat distributions of the anchovy (Engraulis ringens) using the Maxent model in the coastal areas off central-northern Chile. Fisheries Oceanography 28: 171-182.https://doi.org/10.1111/fog.12400

Su HY, Bista MJ, Li MS (2021) Mapping habitat suitability for Asiatic black bear and red panda in Makalu Barun National Park of Nepal from Maxent and GARP models. Scientific reports 11: 14135.https://doi.org/10.1038/s41598-021-93540-x

Subiah HA, Krishna C, Saheli B et al (2018) Synergistic improved efficacy of Gymnadenia orchidis root Salep and pumpkin seed on induced diabetic complications. Diabetes Research and Clinical Practice 146: 278-288.https://doi.org/https://doi.org/10.1016/j.diabres.2018.10.025

Wang YF, Xue K, Hu RH et al (2023a) Vegetation structural shift tells environmental changes on the

Tibetan Plateau over 40 years. Science bulletin 68: 1928-1937.https://doi.org/10.1016/J.SCIB.2023.07.035

Wang YJ, Zhao RX, Zhou XY et al (2023b) Prediction of potential distribution areas and priority protected areas of Agastache rugosa based on Maxent model and Marxan model. Frontiers in Plant Science 14: 1200796.https://doi.org/10.3389/FPLS.2023.1200796

Wang Z, Wang Q, Zhang JK et al (2022) An Integrated Chromatographic Strategy for the Large-Scale Extraction of Ergosterol from Tulasnellaceae sp. Separations 9: 176.https://doi.org/10.3390/SEPARATIONS9070176

Wang ZX, Jia YJ, Li PP et al (2023c) Study on environmental factors affecting the quality of codonopsis radix based on MaxEnt model and all-in-one functional factor. Scientific reports 13: 20726.https://doi.org/10.1038/S41598-023-46546-6

Wei ZQ, Xu ZR, Qiao T et al (2023) Habitats change of Tibetan antelope and its influencing factors on the North Tibetan Plateau from 2020 to 2050. Global Ecology and Conservation 43: e02462.https://doi.org/10.1016/J.GECCO.2023.E02462

Wu TW, Lu YX, Fang YJ et al (2019) The Beijing Climate Center Climate System Model (BCC-CSM): the main progress from CMIP5 to CMIP6. Geoscientific Model Development 12: 1573-1600.https://doi.org/10.5194/gmd-12-1573-2019

Xi YZ, Lang KY, Hu YS (2000) Pollen morphology of Gymnadenia R. Br. (Orchidaceae) and its taxonomic significance. Journal of Systematics and Evolution 38: 137-140.

Xu DP, Zhuo ZH, Wang RL et al (2019) Modeling the distribution of Zanthoxylum armatum in China with MaxEnt modeling. Global Ecology and Conservation 19: e00691.https://doi.org/10.1016/J.GECCO.2019.E00691

Zhang JJ, Jiang F, Li GY et al (2019) Maxent modeling for predicting the spatial distribution of three raptors in the Sanjiangyuan National Park, China. Ecology and Evolution 9: 6643-6654.https://doi.org/10.1002/ece3.5243

Zhao GH, Cui XY, Sun JJ et al (2021) Analysis of the distribution pattern of Chinese Ziziphus jujuba under climate change based on optimized biomod2 and MaxEnt models. Ecological Indicators 132: 108256.https://doi.org/10.1016/j.ecolind.2021.108256

Zheng T, Sun JQ, Shi XJ et al (2022) Evaluation of climate factors affecting the quality of red huajiao

(Zanthoxylum bungeanum maxim.) based on UPLC-MS/MS and MaxEnt model. Food Chemistry: X 16: 100522.https://doi.org/10.1016/J.FOCHX.2022.100522

Zhou QL, Li XF, Wang YC et al (2023a) Mesophytic and less-disturbed mountainous habitats are important for in situ conservation of rare and endangered plants. Global Ecology and Conservation 44: e02488.https://doi.org/10.1016/J.GECCO.2023.E02488

Zhou WY, Li BX, Xu H et al (2023b) Potential distribution of two economic laver species-Neoporphyra haitanensis and Neopyropia yezoensis under climate change based on MaxEnt prediction and phylogeographic profiling. Ecological Indicators 150: 110219.https://doi.org/10.1016/J.ECOLIND.2023.110219

Funding

This work was supported by the Second Tibetan Plateau Scientific Expedition and Research (STEP) program and National Science Foundation of China (grant numbers [2019QZKK0302-02], [31200348], [31971507] and [32001149])

Contributions

Xiujuan Zhang and Junbang Wang, performed study conception and design. Material preparation,data collection and analysis were performed by all authors. The first draft of the manuscript was written by Ming Li, all authors commented on previous of the manuscript. All authors read and approved the final manuscript.

Declaration of Competing Interest

The authors declare that they have no known competing financial interests or personal relationships that could have appeared to influence the work reported in this paper.

Acknowledgements

This work was financially supported by the National Key Research and Development Program of China (2016YFC0500203), National Science Foundation of China (No. 31200348, 31971507; 32001149)

Conflicts of Interest

The authors declare that they have no conflicts of interest.